

The structure of the interstellar gas towards stars in the globular cluster NGC 6541

D.C. Kennedy¹, B. Bates¹, and S.N. Kemp^{1,2}

¹ Department of Pure and Applied Physics, The Queen's University of Belfast, Belfast, BT7 1NN, UK

² Instituto de Astrofísica de Canarias, E-38200 La Laguna, Tenerife, Spain

Received 24 November 1997 / Accepted 21 April 1998

Abstract. Observations are presented of high resolution interstellar Na I D and K I (λ 7699 Å) line profiles towards 7 stars in the globular cluster NGC 6541 and 3 field stars within 3° of the cluster. It is seen that the gas in this general direction ($l, b \sim 350^\circ, -11^\circ$) shows a complex structure, having the greatest number of components yet identified in one of our cluster sightlines, with absorption components detected over an LSR velocity range ~ -100 to $+100$ km s⁻¹. We consider, as far as possible, the identification of the observed gas components. In the low-velocity gas we identify the extensive and nearby diffuse gas which contains the cold, dark and molecular clouds observed closer to the Galactic plane. Components are tentatively identified with both positive and negative peculiar velocity gas components produced by outlying gas in the Sagittarius arm, with gas in the Scutum-Crux and the 3 kpc arms, with an H I filament detected in radio mapping and with shell-like structures expanding from the Sco-Cen association. From the cluster star spectra some variability in the fine scale gas structure is seen on a scale of a few arcsecs.

Key words: ISM: atoms – ISM: clouds – ISM: structure – globular clusters: individual: NGC 6541

1. Introduction

In this paper we present observations of interstellar (IS) Na I D and K I spectral line profiles recorded towards 7 of the brighter stars in the globular cluster NGC 6541 and towards 3 field stars which lie within 3° of the cluster.

The spectra were obtained at the Anglo-Australian Telescope using the University College London echelle spectrograph (UCLES). This report describes a continuation of our studies which are aimed at probing the fine-scale structure and the identification of IS gas components which lie in the foreground of globular clusters. Detailed analyses (including in some cases complementary IRAS, IUE and H I observations) of the structure and properties of the gas have been reported for M 22 (Bates et al. 1992), ω Centauri (Wood & Bates 1993, 1994), M 4 (Kemp et al. 1993), M 55 (Lyons et al. 1994), M 13 (Bates et al. 1995,

Shaw et al. 1996) and M 10 (Kennedy et al. 1996) and references therein.

NGC 6541 has Galactic co-ordinates (l, b) $\approx (349.28^\circ, -11.19^\circ)$ and is at a distance of 7.4 kpc (Harris 1996). This places the cluster at a z -distance below the Galactic plane of ≈ 1.4 kpc. Our observations show that the interstellar gas in the foreground of this cluster has a complex, multi-component structure having the greatest number of components yet identified in one of our cluster sightlines. Using the field star spectra to provide some constraint to component distances, we consider the nature and the origin of the observed components.

2. Observations and data reduction

Observations of 7 stars in NGC 6541 were made during 1994 June 24-27 using UCLES with the 79 grooves mm⁻¹ grating at the 3.9-m Anglo-Australian Telescope. A Tek 1024 \times 1024 CCD was used as detector, and adjacent pixels in the cross-dispersion direction were binned on readout to give a 2-dimensional image of 1024 \times 512 pixels. A slit width of 0.8 arcsec and length of 14 arcsec were used, giving a velocity resolution of ≈ 7.6 km s⁻¹ for the Na I D region and ≈ 7.1 km s⁻¹ for the K I region (instrumental b -values ≈ 4.6 km s⁻¹ and ≈ 4.3 km s⁻¹ respectively) as derived from measurements of the ThAr arc lines. The wavelength setting used was centred on λ 6574 Å in order 34, which provides simultaneous coverage of the Na I D lines and the λ 7699 Å K I line. The identifications and approximate co-ordinates of the cluster stars were made from the finder charts in Alcaïno (1971, 1979), assuming the centre of the cluster to be $\alpha = 18^{\text{h}} 08^{\text{m}} 02.08^{\text{s}}$, $\delta = -43^\circ 42' 19.7''$ (J2000). These finder charts, plus others from CCD images of the centre of NGC 6541 obtained with the 1-m telescope at SAAO in April 1994, were then used to accurately locate the stars during observing. Of the seven cluster stars observed three (hereafter referred to as A, B and C) were recorded simultaneously in the slit. These stars are located near the centre of the cluster field but they have not been formally identified in the over-exposed region of the core of the cluster in the available finding charts. The angular separation (A-B, B-C) of these stars is ≈ 2 arcsec, as deduced from the recorded spectra. The V magnitudes and total exposure times for these stars are listed in Table 1.

Send offprint requests to: B. Bates, (B.Bates@qub.ac.uk)

Table 1. V magnitude and total exposure times (seconds) for the NGC 6541 cluster stars.

Star	V	Exp. Time (s)
A163	12.09	3640
A180	12.44	4500
A71	12.47	4500
A52 (I-21)	12.46	4350
II-21	11.89	2400
I-14	11.29	2000
A,B,C †	-	2000

† - This observation simultaneously recorded the three stars A, B and C in the central region of the cluster.

A further two stars, II-21 and I-14, listed as cluster members in Alcaïno (1979) were observed. However it is clear from their line profiles and anomalous radial velocities that they are not cluster members and they are not considered further in this report. Three stars foreground to NGC 6541 (HD 168905, HD 167756 and HD 163522) were also observed; the V and B magnitudes for these stars, the total exposure times, the central wavelength of the observation, and their angular distances from the cluster centre are listed in Table 2.

Data reduction was performed using the STARLINK package FIGARO (following the methods used in Bates et al. 1993), and CCDPACK (Draper 1993). Normalisation of the continuum and measurements (including error analysis) of the Na I D and K I IS component column densities and radial velocities were performed using the STARLINK package DIPSO (Howarth et al. 1996). The velocities were corrected for the Sun's motion with respect to the dynamical Local Standard of Rest by assuming a solar motion of 16.6 km s^{-1} towards $(l, b) \approx (53^\circ, 25^\circ)$, corresponding to 5.13 km s^{-1} towards NGC 6541.

In addition we make use of an UCLES spectrum of the Ca II region of HD 163522. Details of the observations and reduction are in Smartt et al. (1997).

2.1. Field star distances

Information on the distances and origin of the interstellar gas components detected in the distant cluster star spectra may be obtained from observations of field stars which lie in the general direction of the cluster and at a range of distances. For the NGC 6541 cluster we have observed three field stars. These are well placed relative to the cluster sightline (within 2.1° to 2.9°) but two stars are at distances $\gtrsim 4 \text{ kpc}$ whilst the third (HD 168905) contains no detected interstellar absorption lines and therefore is a relatively nearby star. These above stars are less useful for placing constraints on interstellar component distances than in some of our previous studies of cluster sightlines. For completeness, we consider briefly the field star distances using information from the literature and, where possible, from our spectra.

HD 163522 was classified as a normal B1 Ia by Garrison et al. (1977). Savage et al. (1990) confirm this optical classification

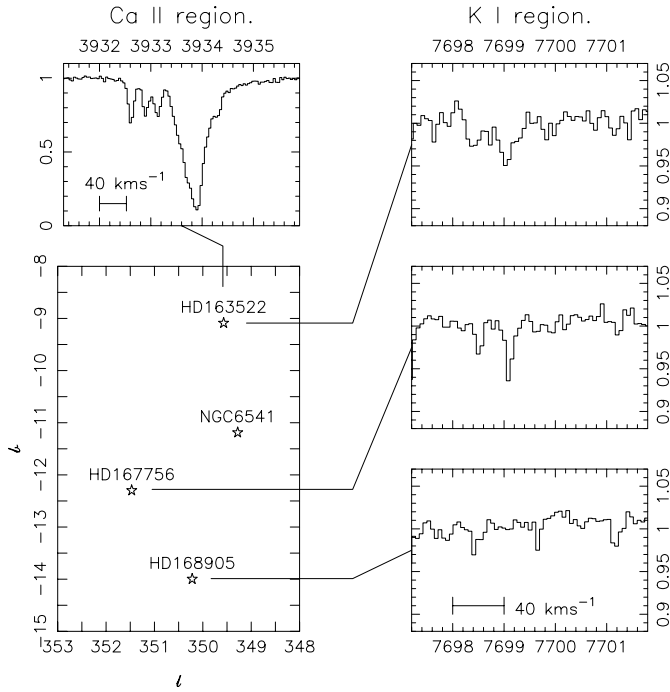
from UV lines, and derive a distance by assigning an absolute magnitude of $M_V = -7 \pm 0.5 \text{ mag}$ based on the Walborn (1972) Population I classification-absolute magnitude calibration. With $E(B - V) = 0.19$ and $A_V/E(B - V) = 3.1$, the estimated distance of HD 163522 is $d = 9.4_{-1.9}^{+2.4} \text{ kpc}$. However, because of its implied location, 1.5 kpc below the Galactic plane, Savage et al. comment that one might suspect that it is not a normal Population I B-supergiant. Smartt et al. (1997) performed a detailed non-LTE analysis of this star and re-classified it as a B1 Ib. They then derive a distance of $5.6 \pm 1.3 \text{ kpc}$ using an absolute visual magnitude for HD 163522 taken from Walborn's calibration, the photometry for this star listed in Sembach et al. (1993) and the $(B - V)_0$ values of Deutschman et al. (1976).

HD 167756 was classified B0.5 Ia by Garrison et al. (1969, 1977) on the basis of high-dispersion optical spectra. Cardelli et al. (1993) verified this optical classification by examining the UV spectrum of the star. Using the line atlases of Lennon et al. (1992, 1993), which present spectra of Galactic blue supergiants from O9.5 - B8, we find that our spectrum of HD 167756, although lacking coverage of many of the more important lines for spectral classification, is consistent with this classification. Using the observed colours of the star ($V = 6.30$, $B - V = -0.13$; Schild et al. 1983) and the intrinsic colours given by Johnson (1963), we derive a colour excess $E(B - V) = 0.09$. We confirm the spectroscopic distance $d = 4.0 \text{ kpc}$ derived by Savage et al. (1994), assuming the absolute magnitude system derived by Walborn (1972) and the relation $A_V = 3.1E(B - V)$.

HD 168905 is classified as B2.5Vn in the SIMBAD database, and Rickard (1974) quotes a distance of 237 pc from UVB photometry. In order to obtain a more reliable estimate of the distance to this star (including a meaningful error range) we have attempted to derive atmospheric parameters using LTE radiative-transfer codes. The stellar gravity was estimated by comparing the observed and theoretical profiles of the $\text{H}\epsilon$ line, which is the most centrally placed across the CCD of any of the Balmer series with our chosen wavelength settings. The $\text{H}\alpha$ line was not considered due to practical difficulties with continuum normalisation and because of the predicted larger non-LTE effects for this line (Auer & Mihalis 1972). The portion of the order containing the $\text{H}\epsilon$ line covers only $\approx 40 \text{ \AA}$ on the CCD and hence both observed and theoretical $\text{H}\epsilon$ profiles were normalised at $\pm 15 \text{ \AA}$ from the line centre. Due to the possible contamination of the blue wing of the $\text{H}\epsilon$ by the stellar He I (3964 \AA) line the fits were primarily constrained by the red wing. This star is a fast rotator; $v \sin i = 297 \text{ km s}^{-1}$ (from the Bright Star Catalogue) was applied to the model line as part of the fitting procedure. The best fit to the $\text{H}\epsilon$ line was obtained with $\log g = 3.8 \pm 0.2$. No suitable temperature sensitive lines (e.g. the Si II/Si III) were available for analysis due either to lack of coverage or a poorly defined continuum. However, *uvby* photometry exists for this star (Ardeberg & Virdefors, 1980), and a $T_{eff} \approx 17450 \text{ K}$ was derived using this photometry and the calibration of Napiwotzki et al. (1993). These stellar parameters (T_{eff} , $\log g$), along with the evolutionary stellar models of Claret & Giménez (1992) yield a distance to HD 168905 of $220_{-45}^{+60} \text{ pc}$.

Table 2. Field star magnitudes, derived distances, Galactic co-ordinates, exposure times, central wavelength and angular distance from the cluster NGC 6541.

Star	<i>V</i>	<i>B</i>	<i>D</i> (kpc)	<i>l</i> (°)	<i>b</i> (°)	Exp. Time (s)	λ (Å)	Ang. Sep. (°)
HD 168905	5.20	5.06	0.2	350.22	-14.00	60	6574	2.9
						120	4239	
						120	4273	
HD 167756	6.30	6.17	4.0	351.47	-12.30	240	6574	2.5
						240	4239	
HD 163522	8.44	8.44	5.6	349.57	-9.09	700	6574	2.1

**Fig. 1.** Relative positions (Galactic coordinates), K I and Ca II (HD 163522 only) line profiles for the 3 field stars observed near NGC 6541. The corresponding velocity scales for each wavelength region are indicated on the line profiles of either HD 163522 or HD 168905. The position of the centre of NGC 6541 is indicated.

The distances derived are summarised in Table 2.

3. Results

The relative positions and interstellar K I line profiles of the cluster and three field stars are displayed in Figs. 1 and 2. The interstellar Na I D line profiles for the cluster and field stars are shown in Figs. 3, 4 and 5. The cluster star spectra reveal stellar Na I D lines blueshifted on average by ≈ -150 km s⁻¹. This places the stellar D₁ line between the interstellar D₂ and D₁ lines.

The numerous telluric lines within the interstellar Na I D region of the line profiles of the program stars were identified and removed by using a scaled template produced from an exposure of a field star, HD 168905. This star was carefully compared with a synthetic telluric spectrum, generated using the data pre-

sented by Lundström et al (1991), and was found to have negligible stellar or interstellar lines in the region of interest. The telluric template produced from HD 168905 gave a better match to the relative strengths of the observed telluric lines than the synthetic spectrum.

A source of profile contamination arises from the Ni I (λ 5892.8 Å) and Ti I (λ 5899.3 Å) stellar lines. Although these lines are weak in the cluster stars due to their Population II membership, they are blueshifted to lie within the interstellar components (Table 5). For example, the blue-shifted Ni I line lies within the negative low-velocity gas components (velocities between ~ -22 to -3 km s⁻¹) of the Na I D₂ line and the displaced Ti I line falls within the positive low-velocity gas components (velocities ~ 1 to 20 km s⁻¹) of the Na I D₁ line. Measurements of the equivalent widths of the Ni I line from our spectra of M15 (metal poor) and M10 (metal rich) yield values ~ 35 and 150 mÅ respectively; the typical width of the lines is ~ 0.2 Å. Towards the cluster NGC 6541, of similar metallicity to M10, profile fitting analysis shows that the effect of the underlying Ni I stellar line on the fits to the observed interstellar components becomes significant for Ni I equivalent widths $\gtrsim 80$ mÅ. Therefore, small differences in the low-velocity gas profiles can be accounted for by small variations of radial velocity of the blue shifted stellar lines and their consequent effect on line blending.

The interstellar Na I D line profiles of the cluster show a complex structure comprising at least 7 components towards some stars. Our results indicate some variability on a scale of only a few arcminutes; in particular the simultaneously recorded stars all lie within a region < 5 arcsecs. However, with the small sample size and the metal line contamination it is difficult to clearly identify any systematic variations across the cluster face. Strong variations are observed in the heavily blended, strong, lower velocity components. Fewer detections are made of the higher velocity gas ($|v| \gtrsim 30$ km s⁻¹). The velocities and strengths of the main component groupings are briefly summarised below. Table 5 illustrates the velocity structure observed in the Na I D region; this table also gives the location of the contaminating stellar Ni I and Ti I lines.

Table 3 lists the velocities ($v_{l,star}$), Na I D and K I logarithmic column densities ($\log N$) and velocity dispersion parameters (b) of the interstellar components detected towards the cluster and foreground stars. Column 1 gives the identification of the stars; the three simultaneously recorded cluster stars are designated A, B and C while the rest of the cluster stars are labelled

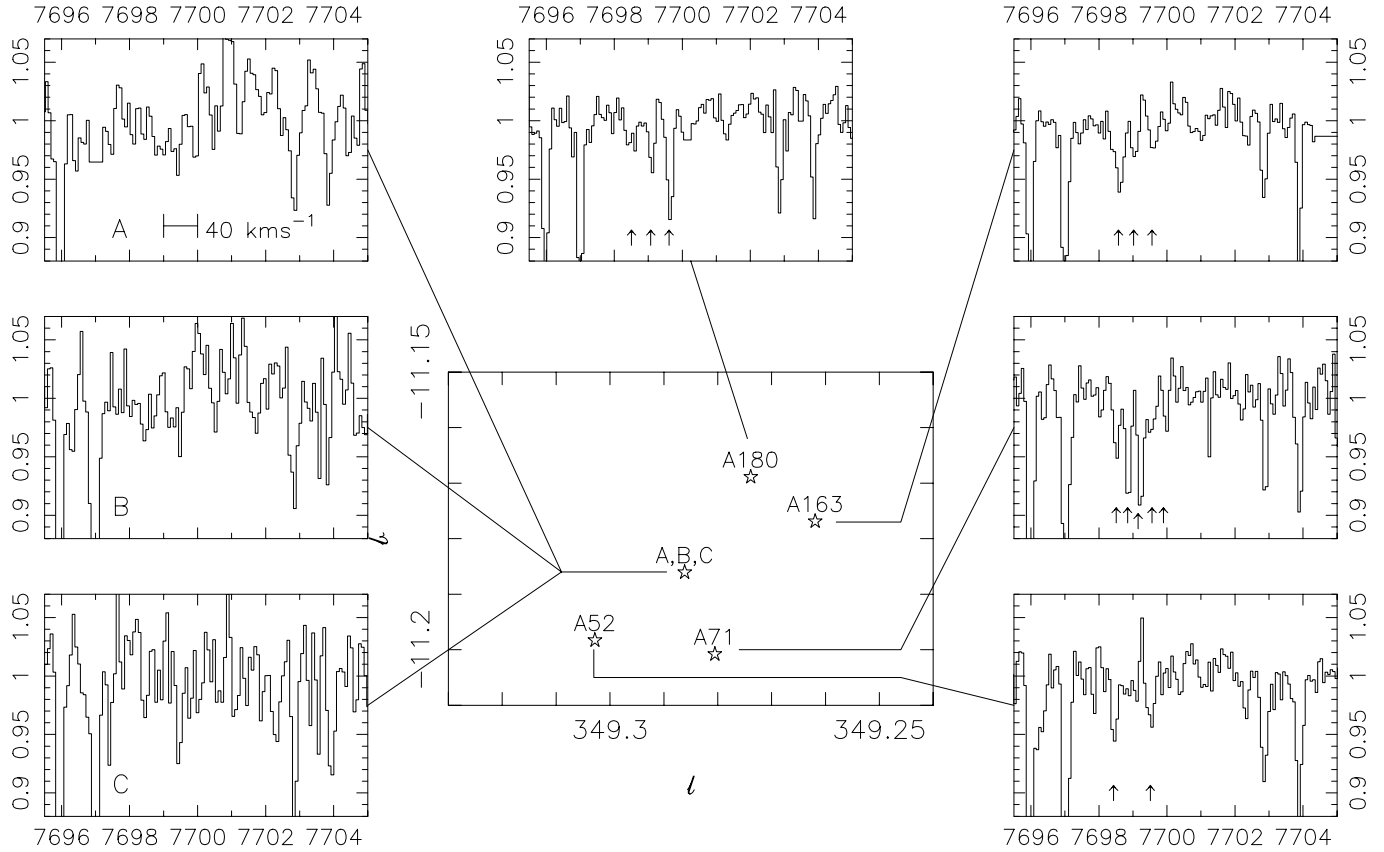


Fig. 2. Relative positions (Galactic coordinates) and normalised K I line profiles for the 7 cluster members observed in NGC 6541. The corresponding velocity scale is indicated on the line profile of the star ‘A’. The positions of the identified interstellar components are marked on the profiles.

according to Alcaino (1971). Columns 2-4 gives the ‘best fit’ velocities, N and b -values for the identified interstellar components. Columns 5-7 and 8-10 give the error ranges on these fit parameters (v_{lsr} , $\log N$, b) for the Na D₂ and Na D₁ regions respectively. Columns 11-15 give the ‘best fit’ parameters and error ranges for the K I region.

The fit parameters were estimated by applying standard profile fitting methods (Wood & Bates 1993) to the lines, and were adjusted until the best fit was obtained between the observed profile and the theoretical profile convolved with the appropriate instrumental broadening function. The unresolved hyperfine components for the Na I D lines were included in the line profile fitting. The errors quoted were determined by judging the range of each parameter that gives an acceptable fit. For narrow (i.e. width dominated by b_{inst}) saturated lines a minimum b value of 0.5 km s^{-1} was adopted. The detection limit for the Na I components is $\log N(\text{Na I}) \approx 10.4$ for the cluster stars, and 10.1 for the field stars.

Table 4 gives similar information for the Ca II lines of the foreground star HD 163522 observed by Smartt et al. (1997).

3.1. Summary of the interstellar components observed

At low positive velocities, between ~ 2 to 7 km s^{-1} , a strong Na I component ($\log N(\text{Na I})$ typically ~ 12.5) is observed to-

wards all cluster stars and towards the field stars HD 163522 and HD 167756. It is also detected in K I towards 3 of the cluster stars, and the two field stars. Another strong component ($\log N(\text{Na I}) \sim 12.3 - 13.0$) is observed at velocities between 20 to 25 km s^{-1} towards all the cluster stars and, more weakly, towards HD 167756. It is also detected in K I towards 4 of the cluster stars.

At low negative velocities, between -15 and -19 km s^{-1} , a strong component ($\log N(\text{Na I}) \sim 12.4$), is observed towards all the cluster stars and HD 167756. This gas is also detected in K I towards 4 of the cluster stars and the field star. A weaker Na I component ($\log N(\text{Na I}) \sim 11.4$) is detected at velocities between -37 to -44 km s^{-1} towards all the cluster stars except A52. A similar component is detected towards HD 163522 at a velocity -50 km s^{-1} . Another weak component ($\log N(\text{Na I}) \sim 11.9$) at a velocity of $\sim 35 \text{ km s}^{-1}$ is detected only towards two cluster stars, A71 and A163. It is observed most clearly, in both Na I and Ca II, towards the field star HD 163522. A blended component ($\log N(\text{Na I}) \sim 11.7$ to 12.8) is also observed at velocities $\approx -5 \text{ km s}^{-1}$ towards all but one (A163) of the cluster stars. This component is not observed towards the field stars, the best Na I fits for the field stars show a similar component at -11 km s^{-1} .

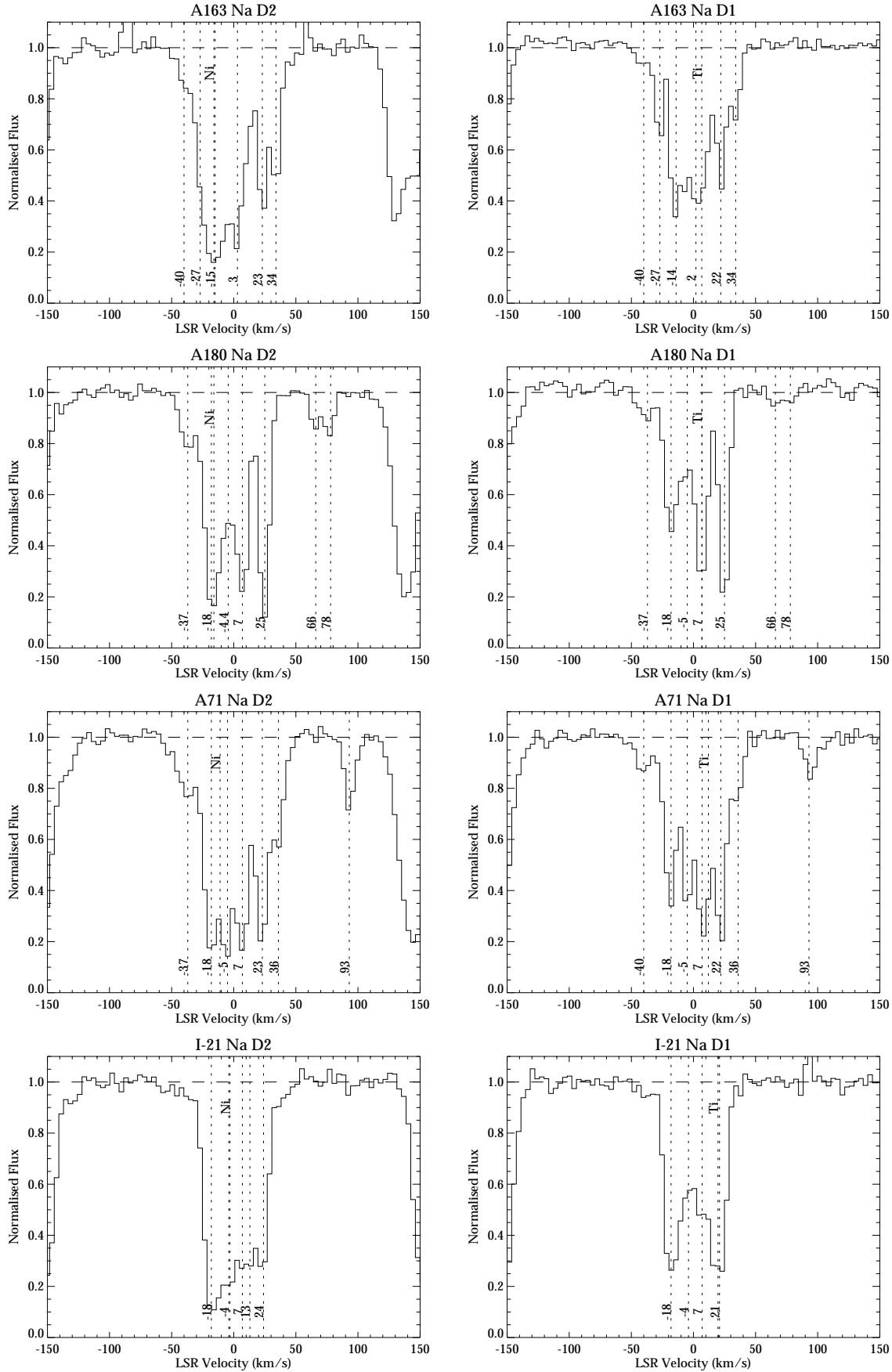


Fig. 3. Na I D line profiles for 4 cluster stars, A163, A180, A71, I-21 (A52). The positions of the fit components are indicated by dotted lines, as are the contaminating Ni I and Ti I stellar lines.

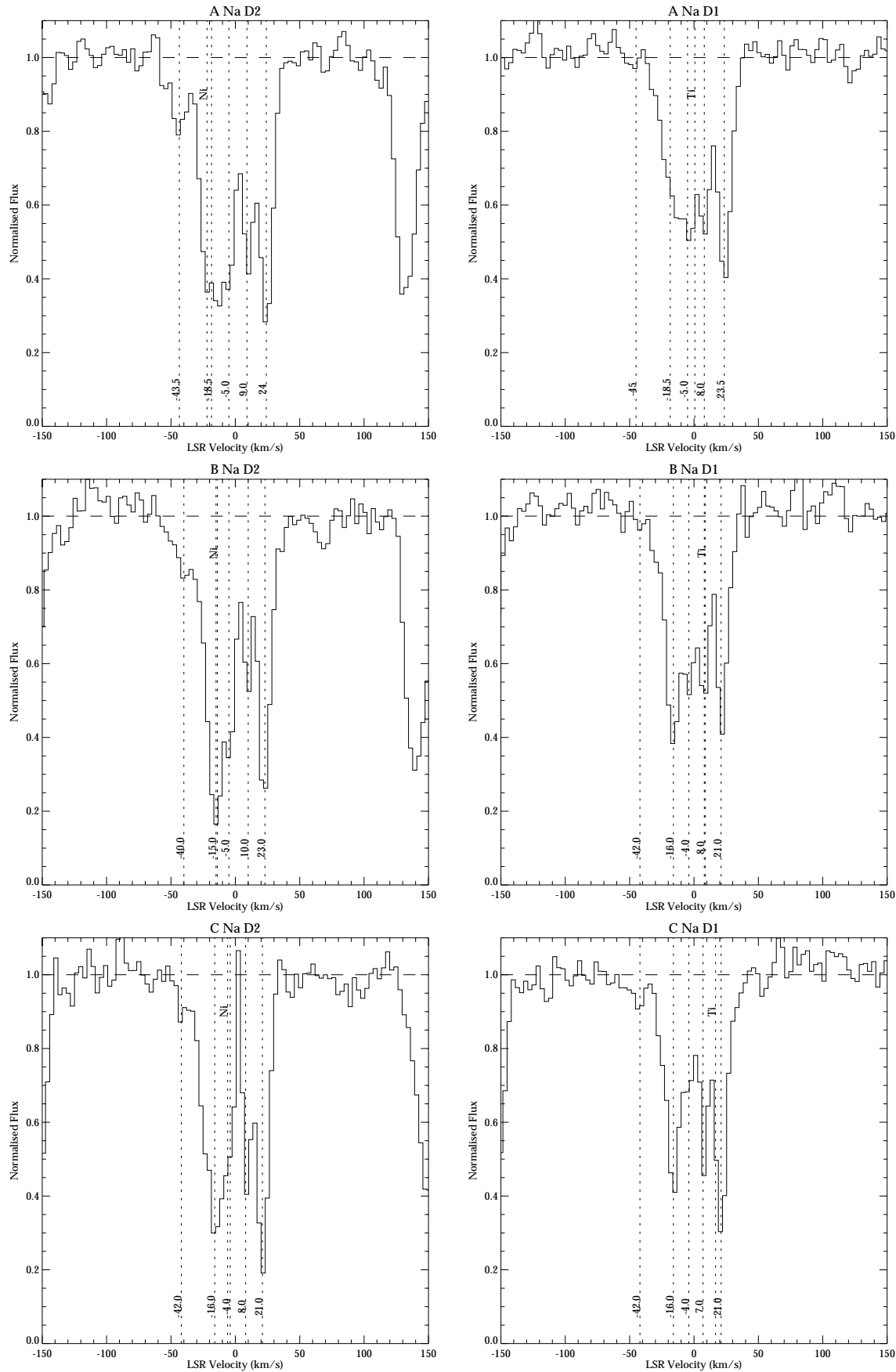


Fig. 4. Na I D line profiles for the three simultaneously recorded cluster stars in NGC 6541; A, B and C. The positions of the fit components are indicated by dotted lines, as are the contaminating Ni I and Ti I stellar lines.

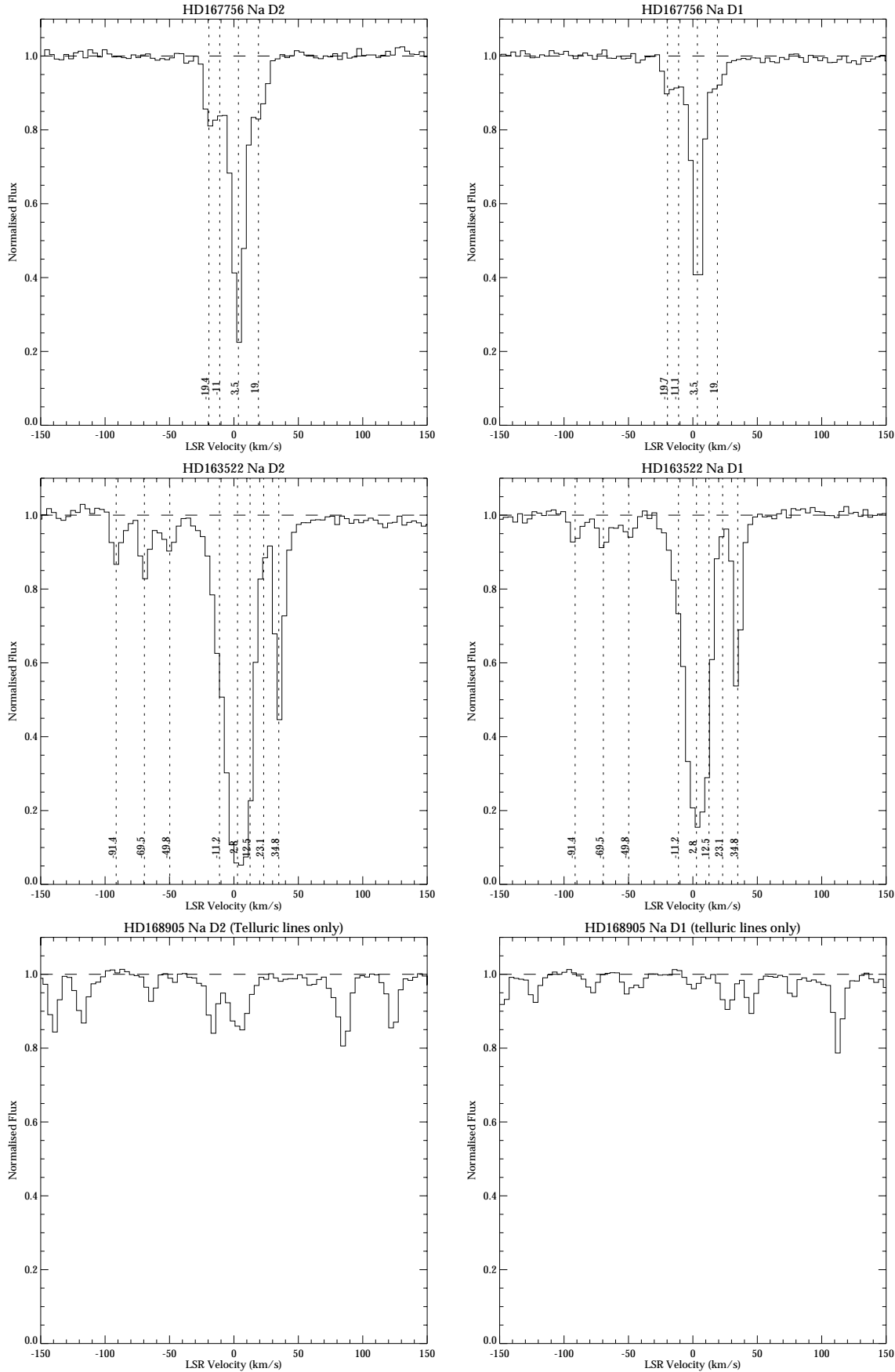


Fig. 5. Na I D line profiles for the three foreground stars towards NGC 6541. The positions of the fit components are indicated by dotted lines. The spectra shown for the stars HD 167756 and HD 163522 have been corrected for telluric lines, which are clearly visible in the HD 168905 line profile.

Table 3. Interstellar Na I D and K I component ‘best fit’ velocities v_{lsr} (km s⁻¹), column densities (N) and b -values, and fit ranges of $\log N$ and b (km s⁻¹) for seven members of the globular cluster NGC 6541, and the two field stars HD 167756 and HD 163522.

Star	Na ‘best fit’			Na I D ₂ fits			Na I D ₁ fits			K I fits				
	v_{lsr}	$\log N$	b	v_{lsr}	$\Delta \log N$	$\Delta \log b$	v_{lsr}	$\Delta \log N$	Δb	v_{lsr}	$\log N$	b	$\Delta \log N$	$\Delta \log b$
A163	-40.0	11.20	3.0	-40.0	11.10-11.23	1.5-5.0	-40.0	11.10-11.30	3.0-6.0				< 10.3	
	-27.0	11.90	2.0	-27.0	11.90-12.50	1.0-3.0	-27.0	11.95-12.50	0.5-2.0				< 10.3	
	-14.5	12.48	6.0	-15.0	12.45-12.55	7.0-9.0	-14.0	12.40-12.50	3.0-5.0	-15.5	10.93	2.0	10.90-11.00	0.5-4.0
	2.5	12.40	6.0	3.0	12.30-12.35	1.0-5.0	2.0	12.45-12.55	7.0-9.0	2.0	10.70	2.0	10.65-1.075	0.5-4.0
	22.5	12.30	2.0	23.0	12.15-14.80	0.5-3.0	22.0	12.40-14.70	0.5-2.0	23.0	10.68	2.0	10.60-10.75	0.5-4.0
	34.0	11.95	2.0	34.0	12.00-14.20	0.5-3.0	34.0	11.80-12.0	1.0-3.0				< 10.3	
A180	-37.0	11.45	5.0	-37.0	11.45-11.50	4.0-6.0	-37.0	11.45-11.50	4.0-6.0				< 10.3	
	-18.0	12.38	5.0	-18.0	12.40-12.42	5.0-6.0	-18.0	12.30-12.35	5.0-6.0	-18.0	10.38	1.0	10.35-10.40	0.5-2.0
	-4.7	11.90	6.0	-4.4	11.85-12.00	5.0-7.0	-5.0	11.90-12.00	5.0-7.0				< 10.3	
	7.0	12.40	3.0	7.0	12.30-12.75	2.0-4.0	7.0	12.45-14.50	1.0-4.0	4.0	10.78	1.0	10.75-10.80	0.5-2.0
	25.0	12.70	3.0	25.0	12.50-14.50	2.0-5.0	25.0	12.60-15.20	1.0-4.0	25.0	11.06	1.0	11.05-11.10	0.5-2.0
	66.0	11.15	1.0	66.0	11.10-11.20	1.0-2.0	66.0	11.00-11.10	1.0-2.0				< 10.3	
	78.0	11.25	2.0	78.0	11.20-11.25	1.0-2.0	78.0	10.80-11.30	1.0-3.0				< 10.3	
A71	-38.5	11.60	7.0	-37.0	11.55-11.65	6.0-9.0	-40.0	11.60-11.70	6.0-8.0				< 10.3	
	-18.0	12.45	4.0	-18.0	12.40-12.50	4.0-5.0	-18.0	12.40-12.70	2.0-4.0	-18.0	10.83	1.0	10.80-10.85	0.5-2.0
	-5.0	12.85	2.0	-5.0	12.40-13.10	2.0-4.0	-5.0	12.40-14.00	1.0-3.0	-5.0	11.05	1.0	11.04-11.10	0.5-2.0
	7.0	12.65	3.0	7.0	12.40-12.50	3.0-4.0	7.0	12.60-12.70	3.0-4.0	7.0	11.12	1.0	11.10-11.15	0.5-2.0
	22.5	12.65	3.0	23.0	12.40-12.50	3.0-4.0	22.0	12.65-15.40	1.0-4.0	23.0	10.52	1.0	10.50-10.55	0.5-2.0
	36.0	11.80	2.0	36.0	11.80-12.30	1.0-3.0	36.0	11.70-11.80	1.0-3.0	36.0	10.63	1.0	10.60-10.65	0.5-2.0
	93.0	11.60	2.0	93.0	11.55-11.70	1.0-4.0	93.0	11.55-11.65	2.0-4.0				< 10.3	
A52	-18.0	12.53	5.0	-18.0	12.50-12.55	5.0-6.0	-18.0	12.55-12.65	5.0-6.0	-21.0	10.85	1.0	10.85-10.90	0.5-2.0
	-4.0	12.20	5.0	-4.0	12.30-12.32	5.0-6.0	-4.0	12.05-12.10	5.0-6.0				< 10.5	
	7.0	12.10	4.0	7.0	11.90-12.00	4.0-5.0	7.0	12.10-12.20	4.0-5.0				< 10.5	
	-	-	-	13.0	11.90-12.10	3.0-6.0							< 10.5	
	22.5	12.35	5.0	24.0	12.20-12.50	2.0-4.0	21.0	12.55-12.60	5.0-6.0	21.0	10.78	2.0	10.75-10.80	0.5-3.0
Centre A	-44.3	11.15	3.0	-43.5	11.40-11.45	3.0-4.0	-45.0	10.80-10.90	1.0-4.0				< 10.8	
	-18.5	12.15	7.0	-18.5	12.20-12.25	7.0-8.0	-18.5	12.10-12.25	7.0-8.0				< 10.8	
	-5.0	12.10	4.0	-5.0	12.05-12.10	4.0-5.0	-5.0	12.10-12.15	3.0-4.0				< 10.8	
	8.5	12.15	2.0	9.0	12.05-12.20	2.0-3.0	8.0	12.10-12.20	2.0-4.0				< 10.8	
	23.8	12.45	2.0	24.0	12.30-12.60	2.0-3.0	23.5	12.32-12.50	2.0-4.0				< 10.8	

Higher velocity ($|v| > 50$ km s⁻¹) components are detected at positive velocities towards 2 cluster stars and at negative velocities towards the field star HD 163522. Towards the cluster star A180 two components are observed at velocities ~ 66 and 78 km s⁻¹ ($\log N(\text{Na I}) \sim 11.1$). A single component of similar strength ($\log N(\text{Na I}) \sim 11.6$) is observed towards A71 at a velocity of 93 km s⁻¹. The negative velocity components towards HD 163522 (velocities ~ -50 , -70 and -91 km s⁻¹, $\log N(\text{Na I}) \sim 11.15$) are observed in both Na I and Ca II.

4. Discussion

The interstellar gas in the foreground of the NGC 6541 cluster shows a complex, multi-component structure and contains by far the largest number of components identified in one of our cluster sightlines. Most of the stronger components are detected in all the cluster star spectra and towards the distant field stars.

Weaker components, in particular those at positive and negative higher velocities, are detected towards fewer stars.

As noted, the two distant stars HD 167756 and HD 163522 lie within 2.5° of the cluster sightline. Detailed discussion of the properties of the gas in these two stellar sightlines, based on UV line profiles, is given in Savage et al. (1994), Cardelli et al. (1995) for HD 167756 and Savage et al. (1990) for HD 163522. Sembach, et al. (1993) present Ca II and Na I profile fits towards both stars. Both sightlines show the existence of absorption lines in the highly ionised species Si IV, C IV and N V produced by gas known to have large scale heights. For the HD 167756 sightline Savage et al. (1994) note that several of the optical components are also detected in the high ions. These authors suggest that the high and low ion gases are not well mixed, though they share some common bulk motions, and discuss the high ion components in terms of conduction fronts at low ion cloud boundaries evaporating or condensing in the pres-

Table 3. (continued)

Star	Na 'best fit'			Na I D ₂ fits			Na I D ₁ fits			K I fits				
	v_{lsr}	$\log N$	b	v_{lsr}	$\Delta \log N$	$\Delta \log b$	v_{lsr}	$\Delta \log N$	Δb	v_{lsr}	$\log N$	b	$\Delta \log N$	$\Delta \log b$
Centre B	-41.0	11.15	3.0	-40.0	11.30-11.45	2.0-3.0	-42.0	10.90-11.00	1.0-2.0				< 10.8	
	-15.5	12.40	6.0	-15.0	12.35-12.50	5.0-6.0	-16.0	12.40-12.45	4.0-5.0				< 10.8	
	-4.5	12.00	2.0	-5.0	11.90-12.20	2.0-3.0	-4.0	12.15-12.70	1.0-2.0				< 10.8	
	9.0	12.30	2.0	10.0	11.85-12.65	1.0-3.0	8.0	12.20-12.30	2.0-3.0				< 10.8	
	22.0	12.60	2.0	23.0	12.50-14.60	1.0-3.0	21.0	12.40-14.13	1.0-3.0				< 10.8	
Centre C	-42.0	11.23	2.0	-42.0	11.10-11.20	2.0-3.0	-42.0	11.30-11.35	1.0-2.0				< 10.8	
	-16.0	12.35	6.0	-16.0	12.30-12.35	7.0-8.0	-16.0	12.35-12.40	5.0-7.0				< 10.8	
	-4.0	11.70	2.0	-4.0	11.60-12.00	1.0-3.0	-4.0	11.70-11.90	1.0-3.0				< 10.8	
	7.0	13.15	1.0	7.0	13.00-13.20	1.0-1.5	7.0	13.00-14.70	0.5-1.0				< 10.8	
	21.0	13.00	2.0	21.0	12.60-14.90	1.0-3.0	21.0	12.60-14.60	1.0-3.0				< 10.8	
HD 167756	-19.6	11.24	2.0	-19.4	11.00-11.35	0.5-2.5	-19.7	11.22-11.25	1.0-2.0	-19.4	10.58	1.0	10.55-10.60	0.5-2.0
	-11.1	11.28	4.0	-11.1	11.27-11.40	0.5-8.0	-11.1	11.23-11.38	2.0-7.0				< 10.3	
	3.5	12.43	3.0	3.5	12.30-13.00	2.0-4.5	3.5	12.35-12.48	2.0-4.5	3.7	10.90	1.0	10.80-10.90	0.5-2.0
	19.0	11.38	6.0	19.0	11.30-11.49	4.0-7.5	19.0	11.25-11.40	3.0-7.0				< 10.3	
HD 163522	-91.4	11.13	1.0	-91.4	11.13-11.14	0.5-2.5	-91.4	11.13-11.14	0.5-2.5				< 10.3	
	-69.5	11.30	1.0	-69.5	11.27-11.30	1.0-2.5	-69.5	11.27-11.30	1.0-2.5				< 10.3	
	-49.8	11.00	3.0	-49.8	10.97-11.05	0.5-4.0	-49.8	10.96-11.05	0.5-4.0				< 10.3	
	-11.2	11.70	3.0	-11.2	11.10-11.75	1.0-7.0	-11.2	11.50-11.90	1.0-7.0				< 10.3	
	2.5	12.90	4.0	2.2	12.60-15.00	3.0-6.0	2.8	12.73-12.85	4.0-6.0	1.5	10.82	2.0	10.78-10.90	0.5-4.0
	12.5	12.18	3.0	12.5	11.30-13.70	1.0-4.5	12.5	12.20-12.22	1.5-4.5				< 10.3	
	23.1	11.03	3.0	23.1	10.80-11.20	1.0-4.0	23.1	10.80-11.10	1.0-3.5				< 10.3	
35.1	12.05	3.0	35.3	11.98-14.56	0.5-3.8	34.8	12.15-12.23	2.0-3.0				< 10.3		

Table 4. Interstellar Ca II K component velocities v_{lsr} (km s⁻¹), and fit ranges of $\log N$ and b (km s⁻¹) for the field star HD 163522. Based on data supplied by Smartt (1997).

v_{lsr}	$\log N$	b
-91.4	11.80-13.10	0.5-4.0
-69.5	11.70-12.60	0.5-4.0
-49.8	11.75-12.65	0.5-5.0
-18.0	12.05-12.15	5.0-10.0
-5.0	12.24-12.35	4.0-7.0
8.0	12.70-12.80	6.0-8.0
23.0	11.90-12.02	2.0-9.0
37.0	11.75-11.95	6.0-11.0

ence of a hotter medium. It is worth noting that Savage et al. (1994) also detect a component at +52 km s⁻¹ in several species (eg. Ca II, Si II, Si IV, C IV) towards HD 167756, however it is not detected in our Na I or K I spectra. Cardelli et al. (1995) find that the sightline to HD 167756 is characterised by warm, low-density diffuse gas of temperatures between 1000 and 5000 K. Relatively high electron densities, more typical of molecule-bearing clouds, suggest some mixing of neutral and ionised gas along the sightline, while there is evidence that some of the low ion absorption like Na I and Ca II may occur in transition regions between neutral and ionised gas.

For the HD 163522 sightline, an analysis of the observed profile shapes given in Savage et al. (1990) shows that they

do not conform with those expected from their models of co-rotating gas. For example, co-rotating gas within 1 to 2 kpc would have a velocity of ~ -5 to -10 km s⁻¹ in the general direction of the NGC 6541 sightline, decreasing to ~ -30 km s⁻¹ at 4 kpc, and -75 km s⁻¹ to -120 km s⁻¹ at 6 to 7 kpc. The analysis of Savage et al. is however based on an estimated stellar distance of 9.4 kpc (co-rotational velocity ~ -145 km s⁻¹). A closer distance of 5.6 kpc (Sect. 2.1) can account more readily for their observed profiles and we consider this further in Sect. 4.5 which reviews the higher velocity components having $|v| > 50$ km s⁻¹.

Danly et al. (1992) show that H I 21-cm emission in the direction of HD 167756 has maximum brightness at +5.5 km s⁻¹ and a broad weak component centred near +30 km s⁻¹. Weak wings of 21-cm emission can be seen to -105 and to +80 km s⁻¹. This star lies at a distance of 4 kpc, and Savage et al. (1994) suggest, from a comparison of H I 21-cm and Lyman- α data, that approximately one-third of the total H I in this direction lies beyond the star.

In the following sections we give a general description of the gas component structure and, where possible, comment on the nature and origin of the components. The reader may find it helpful to refer to Fig. 6 which attempts to summarise schematically the identification, distance and velocity of most of the components.

Table 5. Interstellar gas component velocities determined from the Na D₁ and Na D₂ lines for the 7 cluster stars and two field stars. Also tabulated are the corresponding velocities for the contaminating Ni I and Ti I stellar lines, affecting the Na D₂ and Na D₁ regions respectively.

Star	Velocity km s ⁻¹							Ni I (Na D ₂)	Ti I (Na D ₁)
	-40	-27	-15	3	23	34	66		
A163	-40	-27	-15	3	23	34		-16	7
A180	-37		-18	-5	7	25	66	-16	7
A71	-38		-18	-5	7	23	36	-11	12
A52			-18	-4	7	23		-3	20
A	-44		-19	-5	9	24		-22	1
B	-41		-15	-5	9	22		-14	9
C	-42		-16	-4	7	21		-6	17
HD 167756			-20	-11	4			19	
HD 163522	-91	-70	-50	-11	3	13	23	35	

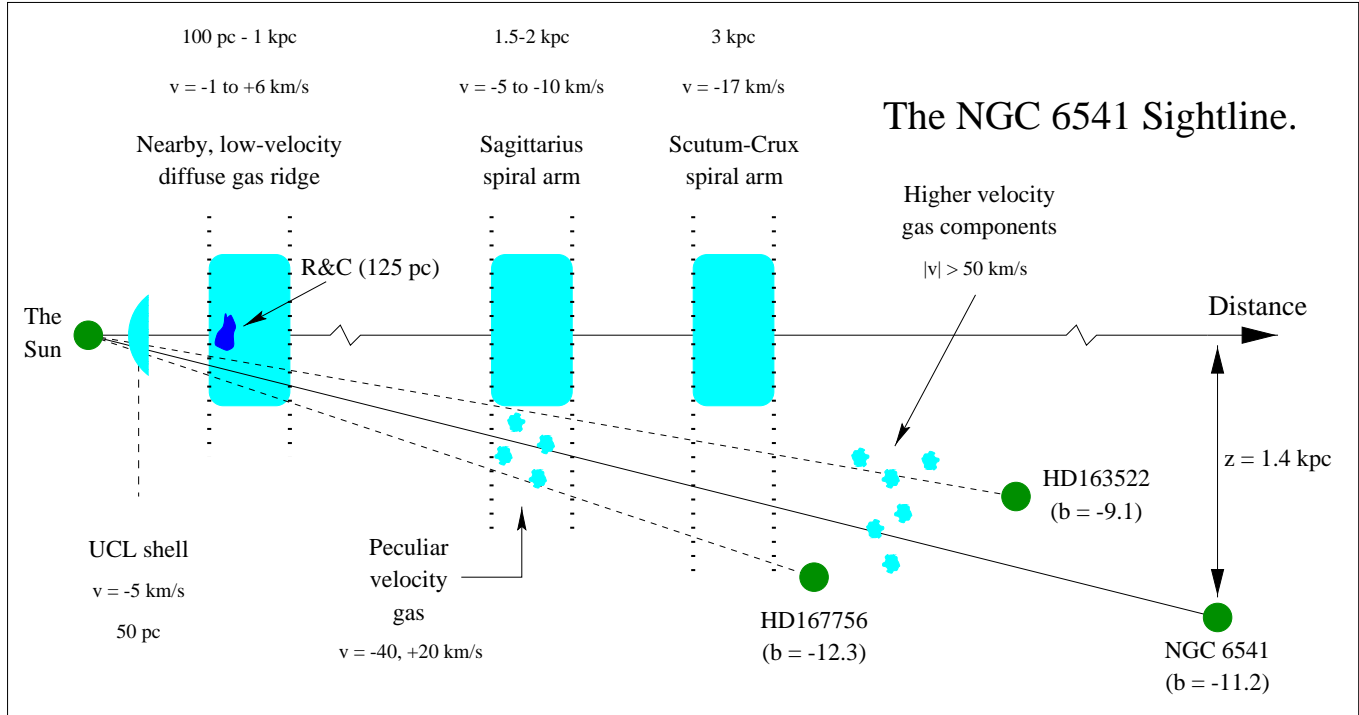


Fig. 6. Schematic diagram for the longitude of the NGC 6541 cluster showing the suggested location of the interstellar gas components in this sightline as discussed in the text. The estimated distances for HD 167756 and HD 163522 are 4.0 kpc and 5.6 kpc respectively.

4.1. Low-velocity gas at $v \sim 5 \text{ km s}^{-1}$

A strong Na I component ($\log N(\text{Na I})$ typically ~ 12.5) is observed towards all cluster stars, HD 163522 and HD 167756 at velocities between ≈ 2 to 7 km s^{-1} . It is also detected in K I towards the cluster stars A163, A180, A71, and towards HD 163522 and HD 167756. This component can be identified with the extensive region of nearby, diffuse gas which contains the Riegel & Crutcher (1972) cold cloud and the molecular and dark clouds which are observed closer to the Galactic plane (Crawford 1992). Detailed observations of a section of the R&C cloud (distance $\sim 150 \text{ pc}$) and its properties are reported in Kemp et al. (1996; and references therein). The cold core of the R&C cloud has been detected in self-absorption in H I radio observations between latitudes -4.2° and $+8^\circ$, at velocities ranging from $+3$ to $+9 \text{ km s}^{-1}$ (Bates et al. 1995). The H I space density of the

cold cloud core is of the order $100\text{-}300 \text{ cm}^{-3}$ and it is thin ($\lesssim 1 \text{ pc}$) in extent (Bates et al. 1995). Outside the approximate latitude range -4° to $+8^\circ$ the H I is detected at similar velocity but only in emission. Previously we have detected this diffuse gas in absorption line spectra of cluster stars observed in M 4 ($l \sim 351^\circ$, $b \sim 16^\circ$, velocity $\sim +3 \text{ km s}^{-1}$), M 10 (15° , 23° , -0.7 km s^{-1}), M 55 (9° , -23° , $+1 \text{ km s}^{-1}$) and M 22 (10° , -7.5° , $+6 \text{ km s}^{-1}$). The NGC 6541 observations add to the spectroscopic studies of the extensive region of nearby, diffuse gas observed in the general direction towards the Galactic centre which has been shown to extend at least from $b \sim +23^\circ$ (Kennedy et al. 1996) to $b \sim -26^\circ$ (Lyons et al. 1994).

4.2. Components at velocities $\sim -40 \text{ km s}^{-1}$, -17 km s^{-1} and $+20 \text{ km s}^{-1}$

A gas component at velocity between ~ 20 to 25 km s^{-1} is clearly seen in each cluster star spectrum and, more weakly, towards HD 167756. The column density towards the cluster stars ranges between $\log N(\text{Na I}) = 12.3$ to 13.0 . This component is also detected in K I, $\log N(\text{K I}) \approx 10.7$, towards 4 cluster stars A163, A180, A71 and A52. At the longitude of NGC 6541, radial velocities for gas participating in Galactic rotation within the solar circle are negative, ranging from ≈ -10 to -60 km s^{-1} for distances from the Sun of 2 and 6 kpc respectively. (Sembach & Danks 1994). In their survey of interstellar material in lower density regions of the Galaxy, Sembach & Danks report that in the longitude range 325° to 0° some 40% of the observed interstellar gas components have ‘forbidden’ positive velocities lying in the range 10 to 50 km s^{-1} .

The origin and distance of the ≈ 20 - 25 km s^{-1} component is essentially unknown, although Savage et al. (1994) suggest a possible link with the Galactic “worms” identified in this area by Koo et al. (1992). However, it is interesting to note that gas components at similar velocity were detected towards M 4 ($l \approx 351^\circ$, $b \approx 16^\circ$) at similar Galactic longitudes in the northern Galactic hemisphere; the M 4 cluster is at a distance of only ~ 2 kpc (Kemp et al. 1993). It is possible that this gas may be outlying gas associated with the Sagittarius spiral arm. Co-rotating gas in the arm would have a velocity of about -5 to -10 km s^{-1} at a distance of 1 to 2 kpc in this direction; the Sagittarius arm in this direction is at an estimated distance of 1.5-2 kpc (Panagia & Tosi 1981). Thus if this component does indeed have an origin in the Sagittarius arm it would have a substantial peculiar velocity. Some support to this possible origin comes from our spectral observations of M 22 and M 55 (Lyons et al. 1994 and references therein) which lie at $l \sim 10^\circ$ and which show similar positive peculiar velocities. A Sagittarius spiral arm distance of 1.5-2 kpc would place the $\sim 20 \text{ km s}^{-1}$ component observed towards NGC 6541 at a z -height of some 280 to 380 pc below the plane. Towards M 55 ($b \sim -23^\circ$) the positive velocity components observed at similar velocity are of much lower column density than is observed towards the clusters closer to the plane. We have noted that a Sagittarius arm origin for the M 55 component implies detection of spiral arm gas some 600 to 800 pc from the plane. The decreasing strength of the peculiar velocity gas components away from the plane may be accounted for by the likely fall off in gas density (Lyons et al. 1994).

The component at velocity $\sim -40 \text{ km s}^{-1}$ is detected towards all of the cluster stars, except for A52, at velocities between -37 to -44 km s^{-1} , and towards the field star HD 163522 at a velocity of -50 km s^{-1} . It is weaker ($\log N(\text{Na I}) \sim 11.4$) than the 20 km s^{-1} velocity component and has greatest strength towards the stars A71 and is weakest towards HD 163522. This component is not detected in K I.

From observations of the interstellar Ca II K line, Rickard (1974) has reported on both negative and positive velocity gas components associated with the Sagittarius arm. Components at negative peculiar velocities are seen towards stars in the lon-

gitude ranges 340° - 0° and 7° - 17° whilst the positive peculiar velocity components are detected mainly in the range 8° - 28° ; the negative peculiar velocity gas components observed between $l = 340^\circ$ - 0° have typical velocities of -35 to -50 km s^{-1} as we observe towards NGC 6541.

Rickard’s sample of stars in the direction $l \sim 350^\circ$ are at latitudes closer to the plane than NGC 6541 and are at estimated distances within ~ 3 kpc. Both the positive and negative components begin at a distance of about 1 kpc and it is seen that most of the peculiar motions are in the Sagittarius spiral arm and not due to gas further away. Our observations towards the more distant NGC 6541 cluster stars do not add further information on the origin of the negative peculiar velocity components.

A strong component, $\log N(\text{Na I}) \approx 12.4$, is observed at velocities between -15 and -19 km s^{-1} towards all the cluster stars and HD 167756. This gas is also detected in K I towards the cluster stars A163, A180, A71, A52 and HD 167756 at velocities between -15 and -21 km s^{-1} . Towards HD 167756 and HD 163522 a less well-defined component at velocity $\sim -11 \text{ km s}^{-1}$, is necessary to achieve a good profile fit.

This -17 km s^{-1} component may possibly originate in the Scutum-Crux spiral arm. Georgelin & Georgelin (1976) define this independent spiral arm in the NGC 6541 direction based upon a survey of H109 α emission and optical H II regions and OB associations. The estimated distance to the Scutum-Crux arm is 3 kpc. At this distance co-rotating gas would have a radial velocity of $\approx -19 \text{ km s}^{-1}$ and the sightline would pass under this arm at $z \sim -650$ pc.

We suggest that turbulent motions of outlying gas in the Sagittarius and Scutum-Crux spiral arms offer a plausible explanation for the origin of the components. Based on our observations of cluster stars, and other material in the literature, this suggestion is more confident in the case of the Sagittarius arm where distances for the components are better determined. A description of the vertical density distribution of H I for Galactic radii 4 to 8 kpc has been given by Dickey & Lockman (1990). The ‘best estimate’ description requires three components of different central density and thickness and is characterised by a resultant density distribution having a FWHM ~ 230 pc. These authors also note that it is possible to lay out a hierarchy of increasing physical temperature (ionisation state) with increasing scale height which ranges from molecular clouds (the species most confined to the plane) through H I and on into the gas traced in highly ionised species such as C IV, Si IV, N V which are known to extend several kpc above the disk. Lockman & Gehman (1991) suggest that the neutral interstellar medium in the solar vicinity is supported in the Galactic gravitational potential primarily by turbulence. There is enough kinetic energy in the H I motion to maintain a layer of FWHM ~ 350 pc; also, about 15% of the H I could be in a component with a scale height ~ 500 pc.

Whilst the origin of these components may lie in turbulent motions within outlying regions of spiral arm gas, the detailed evidence remains incomplete. Further tests would require systematic spectral observations which could determine the variation of gas density and velocity with Galactic latitude in the

spiral arm regions. These might reveal the outer arm density structure and also shed some light on whether gas is detected escaping from or falling back towards the plane.

4.3. Positive velocity gas at $v \sim +35 \text{ km s}^{-1}$

A component at this velocity is detected in Na I in the spectra of two cluster stars (A71, A163) and it is most clearly identified towards the star HD 163522 in both Na I and Ca II spectra.

This gas may also have an origin in the Sagittarius arm where components with similar velocities have been detected towards the M 22 and M 55 clusters (Bates et al. 1992; Lyons et al. 1994). However, in their H I survey, Colomb, Pöppel & Heiles (1980) note the presence of a filament at $l \sim 350^\circ$ which is observed extending from $b \sim -10^\circ$ to -20° . This H I filament has greatest strength at velocity $\sim 38 \text{ km s}^{-1}$ in the Colomb et al. maps. These authors have noted that this feature might be identified with an anomalous-velocity cloud reported by Mirabel & Turner (1975).

From our Na I, Ca II spectra for the star HD 163522 we deduce a component column density ratio $N(\text{Ca II})/N(\text{Na I}) \sim 0.5$. This is in good agreement with the Na I and Ca II data reported for HD 163522 by Sembach et al. (1993). Depending on its distance, the gas has a peculiar velocity of at least 45 km s^{-1} . Sembach & Danks (1994) report on the $N(\text{Ca II})/N(\text{Na I})$ ratio versus absolute peculiar velocity observed for their sample of stars. For a peculiar velocity of $\sim 45 \text{ km s}^{-1}$ their study indicates a corresponding ratio ~ 3 . This is significantly greater than that determined for the $v \sim 35 \text{ km s}^{-1}$ feature in the HD 163522 spectrum. Sembach & Danks (1994) note that it is now generally accepted that the major contribution to the changes in the Ca II/Na I column density ratio occur as a result of the highly variable gas phase abundance of Ca, mostly due to dust processing. The $v \sim 35 \text{ km s}^{-1}$ component detected towards HD 163522 has a Ca II/Na I ratio more consistent with an origin in an H I filament rather than in gas which has been processed destroying dust grains. Certainly this gas has a patchy distribution since, as noted, it is strongest towards HD 163522 and it is detected more weakly towards only two of the cluster stars.

4.4. Negative velocity gas at $v \sim -5 \text{ km s}^{-1}$

The structure of the low-velocity gas is quite complex, comprising several blended components. Analysis of the interstellar profiles towards the cluster stars reveals the presence of a blended component at a velocity $\sim -5 \text{ km s}^{-1}$. This component is variable in strength with $\log N(\text{Na I}) = 11.7$ to 12.8 . However a component at this velocity is not clearly identified in either the HD 167756 or HD 163522 spectra. For these stars, the best fit Na I models indicate a component at $\sim -11 \text{ km s}^{-1}$.

A possible origin for the $\sim -5 \text{ km s}^{-1}$ component is an expanding shell centred on the Sco-Cen association. Crawford (1991) has considered in some detail gas component velocities in relation to expanding shell models using parameters given by de Geus (1992) for the H I shells associated with Sco-Cen. The NGC 6541 sightline would intercept the largest, Upper

Centaurus-Lupus (UCL) shell. The calculated distance to the nearside (approaching) part of this shell based on the Crawford and de Geus models is $\approx 50 \text{ pc}$. Assuming a shell expansion velocity of 7 km s^{-1} as discussed by Crawford, then the predicted shell component velocity in the NGC 6541 direction is $\sim -4.6 \text{ km s}^{-1}$.

4.5. Higher velocity components with $|v| > 50 \text{ km s}^{-1}$

Higher velocity Na I ($|v| > 50 \text{ km s}^{-1}$) components are detected at positive velocities only towards two of the cluster stars and at negative velocity only towards the most distant field star HD 163522. Components are observed at velocity ~ 66 and 78 km s^{-1} ($\log N(\text{Na I}) \sim 11.1$) towards A180 and at 93 km s^{-1} ($\log N(\text{Na I}) \sim 11.6$) towards A71 but they are not detected in the other cluster star sightlines. The negative velocity components (velocities $\sim -50, -70$ and -91 km s^{-1} , $\log N(\text{Na I}) \sim 11.15$) towards HD 163522 are observed in both Na I and Ca II with $N(\text{Ca II})/N(\text{Na I})$ column density ratios > 7 . These positive and negative velocity components are not detected in K I. The Na I component strengths are typically a factor of 10-20 greater than the $3\text{-}\sigma$ detection limit, perhaps implying that the non-detections towards the other sightlines are due to a patchier distribution of the gas rather than a lack of sensitivity in the observations. The non-detection of such higher velocity components towards HD 167756, if not a spatial effect, might imply that their distance is $> 4 \text{ kpc}$. It is possible that these negative higher velocity components observed towards HD 163522 may be associated with the 3 kpc expanding arm in the inner galaxy (Oort 1977). H I maps from Burton (1985, map B183) indicate that at $l = 350^\circ$ H I emission associated with the arm peaks near -110 km s^{-1} , concentrated near the Galactic plane. At the latitude of the cluster sightline the maps show gas in the velocity range ≈ -50 to -100 km s^{-1} . The non-detection of the negative higher velocity components towards the cluster sightline or HD 167756 is simply due to the 3 kpc arm gas being concentrated nearer the Galactic plane.

In their study of the HD 163522 sightline, Savage et al. (1990) estimated a distance to the star of 9.4 kpc . Given this distance they had difficulty explaining the observed higher negative velocity components, which did not conform to their models of co-rotating gas. They had to assume that either there was no halo gas beyond $\approx 6 \text{ kpc}$ or that co-rotation of disk and halo gas stops beyond this distance. This discrepancy is resolved if the revised distance to this star of 5.6 kpc (Smartt et al. 1997, Sect. 2.1) is adopted.

The positive higher velocity gas components detected towards our sample can also be traced in the Burton survey. At positive velocities between $\approx +50$ to $+100 \text{ km s}^{-1}$ the NGC 6541 sightline is shown to contain a thin, clumpy distribution of gas.

Ryans et al. (1997) present Na I and Ca II K interstellar line profiles for a sample of stars lying between $l \sim 350^\circ$ to 16° and at $b \sim -6^\circ$ to -9° . This sample includes HD 163522 and LS 4825. This latter star is of particular interest since it is shown to be a likely young supergiant at a distance of $21 \pm 5 \text{ kpc}$ and hence

on the far-side of the Galaxy. LS 4825 ($l = 1.7^\circ$, $b = -6.6^\circ$) lies some 13° from the cluster and it has a remarkable interstellar gas structure with components detected over a wide velocity range, from -206 to $+93$ km s^{-1} .

The gas components at $v \gtrsim +50$ km s^{-1} are detected only towards LS 4825, the most distant star in the Ryans et al. sample. The authors comment that a plausible explanation for the highest velocity positive and negative components in this sightline is that they represent gas lying within 3 kpc of the Galactic centre where more extreme gas motions are believed to exist. It is quite possible that some of the positive velocity gas components have an origin at considerable distance lying beyond HD 163522 and in the cluster foreground. However as noted, this gas appears patchy in our observations. It may be much closer and not be observed in absorption against the selected target stars due to a purely spatial effect. It is interesting to note the detection of the LS 4825 component at $+93$ km s^{-1} (in Ca II but not Na I) and the Na I component at the same velocity towards the cluster star A71.

5. Summary and conclusions

High resolution Na I D and K I line profiles obtained for 7 stars in NGC 6541 and 3 field stars within 3° show that the gas in the foreground of this cluster has a complex, multi-component structure with absorption components detected over a velocity range ~ -100 to $+100$ km s^{-1} . The field star distances provide little direct information on the distances to the observed gas components. For the cluster stars A, B, and C some variability in the strong low-velocity gas is observed over an angular separation of only ~ 2 arcsecs. High velocity components were only detected towards a few stars, possibly indicating a patchy distribution. A strong low velocity component at $\sim +5$ km s^{-1} is associated with the extensive region of nearby, diffuse gas containing many molecular and dark clouds (Crawford 1992). These present observations extend our studies of this material, including the embedded Riegel & Crutcher (1972) cold cloud, in the general direction towards the Galactic centre. A blended component at ~ -5 km s^{-1} is observed towards all but one of the cluster stars and is consistent with gas originating in an expanding shell centred on the Sco-Cen association identified by Crawford (1991). A strong component at $\sim +20$ km s^{-1} detected towards 8 of our stars is similar to that seen in some of our previous studies (Kemp et al. 1993) and may possibly have an origin in outlying gas associated with the Sagittarius spiral arm. A weaker component at ~ -40 km s^{-1} is detected towards 7 stars in our sample and possibly originates in negative peculiar velocity gas associated with the Sagittarius spiral arm. Another component, at ~ -17 km s^{-1} , is identified towards 8 stars in our sample and is tentatively identified as originating in the Scutum-Crux spiral arm. Towards 3 stars in our sample a component is detected at $\sim +35$ km s^{-1} ; from our data this gas has a $N(\text{Ca II})/N(\text{Na I})$ ratio consistent with its origin in a denser H I filament, possibly that identified in Colomb et al. (1980). Both positive and negative high velocity components ($|v| > 50$ km s^{-1}) are identified in our data. The negative high

velocity gas may be associated with the 3 kpc spiral arm. The origin of the positive high velocity gas remains unclear though comparison is made with the many higher velocity components identified towards the very distant star LS 4825 (Ryans et al. 1997) which lies 13° from the cluster and is thought to be a young supergiant lying on the other side of the Galactic centre.

Acknowledgements. We are grateful for the observational support provided by the staff at the AAT. Financial support has been provided by the Particle Physics & Astronomy Research Council; DCK acknowledges receipt of a Department of Education Northern Ireland research studentship. We especially wish to thank Dr. Stephen Smartt for his assistance with stellar distances and for his Ca II data.

References

- Alcaino G., 1971, *A&A* 13, 399
 Alcaino G., 1979, *A&AS* 35, 233
 Ardeberg A., Virdefors B., 1980, *A&AS* 40, 307A
 Auer L. H., Mihalis D., 1972, *ApJS* 24, 193
 Bates B., Montgomery A.S., Wood K.D., Walker H.J., 1992, *MNRAS* 257, 699
 Bates B., Kemp S.N., Montgomery A.S., 1993, *A&AS* 97, 937
 Bates B., Shaw C.R., Kemp S.N., Keenan F.P., Davies R.D., 1995, *ApJ* 444, 672
 Bates B., Montgomery A.S., Kemp S.N., 1995, *MNRAS* 277, 811
 Burton W.B., 1985, *A&AS* 62, 365
 Cardelli J.A., Ebbets D.C., Savage B.D., 1993, *ApJ* 412, 401
 Cardelli J.A., Sembach K.R., Savage B.D., 1995, *ApJ* 440, 241
 Claret A., Giménez A., 1992, *A&AS* 96, 255
 Colomb F.R., Pöppel W.G.L., Heiles C., 1980, *A&AS* 40, 47
 Crawford I.A., 1991, *A&A* 247, 183
 Crawford I.A., 1992, *MNRAS* 254, 264
 Danly L., Lockman F.J., Meade M.R., Savage B.D., 1992, *ApJS* 81, 125
 Dickey J.M., Lockman F.J., 1990, *ARA&A* 28, 215
 Draper P.W., PPARC Starlink User Note, 139.3, 1993, DRAL/Rutherford Appleton Laboratory
 Deutschman W.A., Davies R.J., Schild R.E., 1976, *ApJS* 30, 97
 Garrison R.F., Hiltner W.A., Schild R.E., 1969, *A&A* 157, 313
 Garrison R.F., Hiltner W.A., Schild R.E., 1977, *ApJS* 35, 111
 Georgelin Y.M., Georgelin Y.P., 1976, *A&A* 49, 57
 de Geus E.J., 1992, *A&A* 262, 258
 Harris W.E., 1996, *AJ* 112, 1487
 Howarth I.D., Murray J., Mills D., Berry D.S., 1996, DIPSO (V3.4) - A Friendly Spectrum Analysis Program, Starlink User Note 50.20 (Chilton, UK: Rutherford Appleton Lab.)
 Johnson H.L., 1963, in *Stars and Stellar Systems*, 3, Basic Astronomical Data, ed. K. A. Strand (Chicago: Univ. of Chicago Press), 214
 Kemp S.N., Bates B., Lyons M.A., 1993, *A&A* 278, 542
 Kemp S.N., Bates B., Hambly N.C., 1996, *MNRAS* 283, 1089K
 Kennedy D.C., Bates B., Kemp S.N., 1996, *A&A* 309, 109
 Koo B.C., Heiles C., Reach W.T., 1992, *ApJ* 390, 108
 Lennon D.J., Dufton P.L., Fitzsimmons A., 1992, *A&AS* 94, 569
 Lennon D.J., Dufton P.L., Fitzsimmons A., 1993, *A&AS* 97, 559
 Lockman F.J., Gehman C.S., 1991, *ApJ* 382, 182
 Lundström I., Ardeberg A., Maurice E., Lindgren H., 1991, *A&AS* 91, 199 Lyons M.A., Bates B., Kemp S.N., 1994, *A&A*, 286, 535
 Mirabel I. F., Turner K.C., 1975, *Ap&SS* 38, 381
 Napiwotzki R., Schöberner D., Wenske V., 1993, *A&A* 268, 653

- Oort J., 1977, *ARA&A* 15, 295
Panagia N. Tosi M., 1981, *A&A* 96, 306
Rickard J.J., 1974, *A&A* 31, 47
Rickard J.J., 1975, *A&A* 41, 403
Riegel K.W., Crutcher R.M., 1972, *A&A* 18, 55
Ryans R.S.I., Dufton P.L., Keenan F.P., et al. 1997, *ApJ* 490, 267
Savage B.D., Massa D., Sembach K.R., 1990, *ApJ* 355, 114
Savage B.D., Sembach K.R., Cardelli J.A., 1994, *ApJ* 420, 183
Schild R. E., Garrison R.F., Hiltner W.A., 1983, *ApJS* 51, 321
Sembach K.R., Danks A.C., 1994, *A&A* 289, 539
Sembach K.R., Danks A.C., Savage B.D., 1993, *A&AS* 100, 107
Shaw C.R., Bates B., Kemp S. N., et al., 1996, *ApJ* 473, 849
Smartt S.J., Dufton P.L., Lennon D.J., 1997, *A&A* 326, 763
Walborn N.R., 1972, *AJ*. 77, 4
Wood K.D., Bates B., 1993, *ApJ* 417, 572
Wood K.D., Bates B., 1994, *MNRAS* 267, 660